

# Recovery of spectral sensitivity functions from a colour chart image under unknown spectrally smooth illumination

Cong Phuoc Huynh<sup>1,2</sup> Antonio Robles-Kelly<sup>1,2,3</sup>

<sup>1</sup> NICTA , Locked Bag 8001, Canberra ACT 2601, Australia

<sup>2</sup>Research School of Engineering, ANU, Canberra ACT 0200, Australia

<sup>3</sup>School of Eng. and Inf. Tech., UNSW@ADFA, Canberra ACT 2600, Australia

**Abstract**—This paper proposes a method to approximate the camera spectral sensitivity functions from a single colour image of a colour chart under an unknown illumination spectrum. Here we assume that the scene illumination has a smooth spectral variation. Although the original problem is rather ill-posed, we reformulate it as a well-posed optimisation one by introducing several constraints. The first constraint concerns with the smoothness of the illuminant power spectrum. The second one is based on the fact that the spectral sensitivity function of a digital camera should be constrained to a linear subspace according to Luther condition. The third constraint limits the influence of bands with low signal-to-noise ratios. By introducing these constraints, we can solve the problem in a coordinate-descent optimisation manner. We validate our method using data acquired from over 40 commercial camera models and compare with an alternative in the literature. We also demonstrate the utility of the estimated colour matching functions for colour simulation and colour transfer.

## I. INTRODUCTION

In computer vision, the accurate capture and reproduction of colours acquired by digital camera sensors has applications in colour correction [1], [2], camera simulation [3] and sensor design [4]. It is often assumed that the spectral sensitivity of trichromatic imaging sensors to incoming light abides to the CIE color matching functions [5]. This assumption is important since colorimetric standards are, by definition, device independent. However, this may not be the case in practice as the spectral sensitivity functions of digital cameras can differ greatly from the CIE standards [6], [7].

Nonetheless it is somewhat well known that it is possible to recover the spectral response of a particular camera using narrow band illuminants, calibration targets and charts. Existing methods employ photogrammetry and spectroscopy techniques to recover the spectral response of the camera under study [8]. Several methods for colorimetric simulation and evaluation with measurements of material reflectance and illuminant radiance have been proposed, through the use of tools such as quadratic programming [9], monochromators [10], spectrophotometers [11] or fluorescence [12].

Other methods elsewhere in the literature require the scene radiance to be in hand [13] or make a particular assumption regarding the scene. For instance, in [14], the authors assumed the sky is visible and employed this assumption to recover the spectral sensitivity function of the camera. As a result, existing

methods are often restricted to complicated acquisition setups or strong assumptions on either the illuminant power spectrum or the scene irradiance. In practice, this is often restrictive since the user only has at his/her disposal a color checker whose image has been acquired under a particular illuminant.

In such a situation, we note that the recovery of the spectral sensitivity functions is ill-posed in a strict sense [15]. Nonetheless, the spectral sensitivity functions can be approximated using a single image from a colour rendition chart, *i.e.* an XRite ColorChecker chart captured under an unknown illuminant covering the full extent of the visible spectrum and a library of reflectances acquired a priori. This setting allows for a method with the following assumptions

- The use of illuminants with smooth spectra such as incandescent lamps, tungsten lights or sunlight.
- A uniformly illuminated colour rendition chart of known shape.
- Known spectral reflectance for the colour patches in the chart.

Although the method presented here is somewhat related to the work presented in [13] and [15], it has noticeable differences. In contrast with [15], it does not require a known illumination spectrum. Moreover, it employs iterative optimisation instead of a search over the range of illuminant colour temperatures as in [15]. To this end, we assume that the illuminant power spectrum is smooth across the wavelengths and impose a spectral smoothness constraint on the camera sensitivity function. Furthermore, we note that the camera sensitivity functions should obey Luther condition [16] in order to correctly reproduce the colours perceived by the human eye. Hence, they lie on a subspace spanned by a linear basis. We further constrain the optimisation by limiting the influence of bands with low signal-to-noise ratios.

The paper is structured as follows. In Section II, we introduce an image formation model with relevant notation. Based on this model, we propose a coordinate-descent optimisation approach in Section III, where the spectral sensitivity functions and the illumination power spectrum are estimated in alternating steps. In Section IV, we validate the accuracy of our method in comparison to an alternative, and illustrate its utility for colour simulation and colour transfer. Finally, we draw conclusions on this work in Section V.

## II. IMAGE FORMATION MODEL

In the setting of this work, we are given an input image consisting of  $m$  pixels denoted as  $u_1, \dots, u_m$ . Our objective is to recover the illumination spectrum and the spectral sensitivity of the sensors at discretely sampled wavelengths  $\lambda_1, \dots, \lambda_n$ . Let  $I_c(u)$  be the colour value for channel  $c \in \{R, G, B\}$  at pixel  $u$ . Here, we consider a scene with a global illuminant power distribution  $L(\lambda)$ , where  $\lambda$  denotes the wavelength. In addition, let  $S(u, \lambda)$  be the surface reflectance at pixel  $u$  and wavelength  $\lambda$ , and  $Q_c(\lambda)$  be the spectral sensitivity of the colour channel  $c$  at wavelength  $\lambda$ .

Further, let  $\mathbf{I}_c$  be the colour vector for channel  $c$  formed by concatenating  $I_c(u)$  over all the image pixels. In addition, we define the illumination power spectrum  $\mathbf{L}$  as  $\mathbf{L} \triangleq [L(\lambda_1), \dots, L(\lambda_n)]^T$  and the spectral reflectance spectrum at an image pixel  $u$  as  $\mathbf{S}(u) \triangleq [S(u, \lambda_1), \dots, S(u, \lambda_n)]^T$ . Building on this notation, we can construct a matrix of reflectance spectra over all the image pixels,  $\mathbf{S} = [\mathbf{S}(u_1), \dots, \mathbf{S}(u_m)]^T$ . Also, in the discrete spectral domain, the spectral sensitivity function for the colour channel  $c$  can be described as a vector  $\mathbf{Q}_c = [Q_c(\lambda_1), \dots, Q_c(\lambda_n)]^T$ .

Here, we depart from the image formation model of colour images to relate the input image to the illuminant power spectrum, the scene reflectance and the spectral sensitivity of the imaging sensor. According to [7], the colour value for a single channel  $c \in \{R, G, B\}$  at pixel  $u$  is an integration over the visible spectrum  $V = [400nm, 780nm]$ , as follows

$$I_c(u) = s_c \int_V Q_c(\lambda) L(\lambda) S(u, \lambda) d\lambda, \quad (1)$$

where  $s_c$  corresponds to the white balancing factor in channel  $c$ . Note that, we can rewrite Equation 1 in the matrix form as the following expression

$$\mathbf{I}_c = s_c \mathbf{S}(\mathbf{L} \odot \mathbf{Q}_c), \quad (2)$$

where  $\odot$  stands for the element-wise multiplication.

## III. OPTIMISATION PROBLEM

We assume that the colour chart under consideration has known spectral reflectance. The reflectance can be measured beforehand using either a spectrometer or a hyperspectral camera. This can be done in a straightforward manner by capturing a hyperspectral image of the chart under arbitrary lighting. Since the illuminant power spectrum is deemed to be the radiance spectra at the white colour patch on the chart, the reflectance of the entire chart can then be obtained by taking the ratio of the spectral radiance to the illumination power spectrum.

We recover the spectral sensitivity function with a two-stage algorithm. In the first stage, given the known scene reflectance matrix  $\mathbf{S}$ , we estimate the element-wise product  $\mathbf{P}_c$ , where  $\mathbf{P}_c \triangleq s_c \mathbf{L} \odot \mathbf{Q}_c$  for the colour channel  $c$ . By Equation 2, we can recover  $\mathbf{P}_c$  by solving the following non-negative linear optimisation problem

$$\begin{aligned} & \text{minimise} \quad \|\mathbf{I}_c - \mathbf{S}\mathbf{P}_c\| \\ & \text{subject to} \quad \mathbf{P}_c \succ \mathbf{0}, \end{aligned} \quad (3)$$

where  $\|\cdot\|$  denotes the  $L^2$ -norm of the vector argument.

We observe that there are  $n$  variables in  $\mathbf{P}_c$  corresponding to the  $n$  discrete wavelengths  $\lambda_1, \dots, \lambda_n$ . Since  $\mathbf{S}$  has a dimension of  $m \times n$ , the problem in Equation 3 is generally well-formed if there are more pixels in the image than the number of wavelengths, i.e.  $m \geq n$ . As a result, the minimisation above can be solved by standard non-negative least squares methods [17].

In the second stage, having obtained the vectors  $\mathbf{P}_c, c \in \{R, G, B\}$ , we aim to decompose them into the illuminant power spectrum  $\mathbf{L}$  and the spectral sensitivity function  $\mathbf{Q}_c$ . We note that the decomposition problem above is ill-posed without further constraints. In other words, for any illuminant power spectrum  $\mathbf{L}$ , there always exists a spectral sensitivity function  $\mathbf{Q}_c$  such that  $\mathbf{Q}_c \odot \mathbf{L}$  is a scalar multiple of  $\mathbf{P}_c$ . To tackle the ambiguity induced by the unknown scalar  $s_c$  in Equation 2, here we minimise the spectral angle  $\angle(\mathbf{P}_c, \mathbf{Q}_c \odot \mathbf{L})$  between the vectors  $\mathbf{P}_c$  and  $\mathbf{Q}_c \odot \mathbf{L}$ . Moreover, we constrain the vectors  $\mathbf{Q}_c$  and  $\mathbf{L}$  to unit  $L^2$ -norm.

To render the above problem well-formed, we assume that both the illumination power spectrum and the spectral sensitivity functions are smooth in the spectral domain. These assumptions have been employed elsewhere for material end member decomposition in spectral unmixing [18] and spectral sensitivity recovery [13]. These works, in particular, model local segments of the spectra as linear functions. Therefore, they constrain the spectra such that the magnitude of the second derivatives with respect to the wavelength is minimised.

In the discrete form, the second derivative of spectra can be approximated by finite differences with the following  $(n-2) \times n$  matrix

$$\mathbf{D} = \begin{pmatrix} 1, -2, 1, 0, \dots, 0 \\ 0, 1, -2, 1, \dots, 0 \\ \vdots \\ 0, \dots, 0, 1, -2, 1 \end{pmatrix}, \quad (4)$$

which is a band matrix with non-zero entries on the main diagonal and its two adjacent upper diagonals.

With this band matrix in hand, the magnitudes of the second derivatives of the illumination spectrum  $\mathbf{L}$  and the spectral sensitivity  $\mathbf{Q}_c$  can be approximated as follows

$$\int \left( \frac{\partial^2 L(\lambda)}{\partial \lambda^2} \right)^2 d\lambda \approx \|\mathbf{D}\mathbf{L}\|^2 \quad (5)$$

$$\int \left( \frac{\partial^2 Q_c(\lambda)}{\partial \lambda^2} \right)^2 d\lambda \approx \|\mathbf{D}\mathbf{Q}_c\|^2. \quad (6)$$

In addition, we constraint the spectral sensitivity function making use of Luther's condition [16]. This condition states that, in order to reproduce colour accurately, the spectral sensitivity function of a camera should be a linear combination of the human eye's colour matching functions. Several prior works [19], [15] have empirically verified that the spectral response functions of digital cameras span a low-dimensional linear subspace. This experimental work spans a wide variety of pre-defined linear basis functions such as polynomials, Fourier series, radial basis functions and the principal components obtained by PCA.

For now, we assume a pre-defined basis  $\mathcal{B}_c$  of the spectral sensitivity functions in each channel  $c$ . To enforce a linear basis for the sensitivity function  $\mathbf{Q}_c$ , we define a distance metric between the sensitivity function  $\mathbf{Q}_c$  and the subspace spanned by  $\mathcal{B}_c$ . To this end, we concatenate the column vectors that represent the components in  $\mathcal{B}_c$  to form a matrix  $\mathbf{B}_c$  with a size of  $n \times d_q$ , where  $d_q$  is the number of basis components in  $\mathcal{B}_c$ . The linear projection matrix onto this subspace is given by  $\mathbf{B}_c \mathbf{B}_c^\dagger$ , where  $\dagger$  denotes the pseudo-inverse of a matrix. With these ingredients, we proceed to define the distance  $d(\mathbf{Q}_c, \text{span}(\mathcal{B}_c))$  between the sensitivity function  $\mathbf{Q}_c$  and the subspace spanned by  $\mathcal{B}_c$  as the difference between its projection onto this subspace and itself, i.e.  $d(\mathbf{Q}_c, \text{span}(\mathcal{B}_c)) = \|\mathbf{T}_c \mathbf{Q}_c\|$ , where  $\mathbf{T}_c \triangleq \mathbf{J} - \mathbf{B}_c \mathbf{B}_c^\dagger$  and  $\mathbf{J}$  is the identity matrix.

Lastly, we notice that the spectral sensitivity is only significant in a number of wavelengths, i.e. it peaks at a certain wavelength and falls off at the tails. This gives rise to a constraint on the sensitivity values of the insignificant bands, which we define to have values below a certain proportion of the maximum value of the function. Formally, we denote the significance of the wavelength  $\lambda$  for each channel  $c$  as an indicator function  $w_c(\lambda)$ . We preset the value of  $w_c(\lambda)$  as follows

$$w_c(\lambda) = \begin{cases} 0, & \text{if } P_c(\lambda) < \epsilon \times \max_{\lambda' \in V} P_c(\lambda') \\ 1, & \text{otherwise,} \end{cases} \quad (7)$$

where  $P_c(\lambda)$  is the element of  $\mathbf{P}_c$  at the wavelength  $\lambda$  and  $\epsilon$  is a preset constant.

Subsequently, we construct a significance indicator vector  $\mathbf{w}_c$  over the wavelength domain for each colour channel  $c$ . This allows for an appropriate weighting of bands based on their signal-to-noise ratios by minimising the norm  $\|(\mathbf{1} - \mathbf{w}_c) \odot \mathbf{Q}_c\|^2$ , where  $\mathbf{1}$  is the  $n$ -element column vector of unit values and  $\mathbf{w}_c = [w_c(\lambda_1), \dots, w_c(\lambda_n)]^T$ .

By combining all the constraints above, we formulate the problem of decomposing  $\mathbf{P}_c$  into  $\mathbf{L}$  and  $\mathbf{Q}_c$  as the following minimisation problem

$$\begin{aligned} \text{minimise } F = & \left\{ \sum_c \mathcal{L}(\mathbf{P}_c, \mathbf{Q}_c \odot \mathbf{L}) + \alpha_L \|\mathbf{D}\mathbf{L}\|^2 \right. \\ & + \alpha_Q \|\mathbf{D}\mathbf{Q}_c\|^2 + \beta_Q \|\mathbf{T}_c \mathbf{Q}_c\|^2 \\ & \left. + \gamma_Q \|(\mathbf{1} - \mathbf{w}_c) \odot \mathbf{Q}_c\|^2 \right\} \\ \text{subject to } & \|\mathbf{Q}_c\| = 1 \text{ and } \|\mathbf{L}\| = 1, \end{aligned} \quad (8)$$

where  $\alpha_L, \alpha_Q, \beta_Q, \gamma_Q$  are the corresponding Lagrange multipliers for the constraints introduced above.

Subsequently, we employ a coordinate descent method to minimise the cost function in Problem 8. Specifically, we refine the estimates of the spectral sensitivity function and the illumination power spectrum in an iterative manner. At each iteration, we minimise the cost function in Problem 8 in two interleaved steps, each with respect to either  $\mathbf{L}$  or  $\mathbf{Q}_c$  while fixing the update of the other variable. To optimise the objective function at each step, we employ the interior point algorithm for large scale non-linear programming described in [20].

---

**Algorithm 1** Estimate the spectral sensitivity function  $\mathbf{Q}_c, c \in \{R, G, B\}$  and the illumination power spectrum  $\mathbf{L}$ .

---

**Require:**  $\mathbf{P}_c$ : the scalar multiple of the element-wise product of  $\mathbf{Q}_c$  and  $\mathbf{L}$  obtained by solving Problem 3.

- 1: Initialise  $t \leftarrow 0$ ;  $\mathbf{L}^{(0)} \leftarrow \mathbf{1}$ .
  - 2: **repeat**
  - 3:   **for**  $c \in \{R, G, B\}$  **do**
  - 4:      $\mathbf{Q}_c^{(t)} \leftarrow \text{argmin}_{\mathbf{Q}_c} F|\mathbf{L}^{(t-1)}$ .
  - 5:   **end for**
  - 6:    $\mathbf{L}^{(t)} \leftarrow \text{argmin}_{\mathbf{L}} F|\mathbf{Q}_c^{(t)}$ .
  - 7:    $t \leftarrow t + 1$ .
  - 8: **until** the change in  $\mathbf{L}^{(t)}, \mathbf{Q}_c^{(t)}$  as compared to the previous iterates is negligible or the maximum number of iterations is reached.
  - 9: **return**  $\mathbf{L}^{(t)}, \mathbf{Q}_c^{(t)}$ .
- 

In Algorithm 1, we present the pseudocode for our method. In the algorithm, the superscript  $t$  denotes the iteration index. The algorithm takes the solution  $\mathbf{P}_c$  resulting from the minimisation problem 3 as input and commences with an initialisation of the illumination power to a uniform spectrum. The algorithm terminates when the changes in the illumination spectrum and the sensitivity function estimates are negligible, or a maximum number of iterations is achieved.

#### IV. EXPERIMENTS

In this section, we first evaluate our method for spectral sensitivity estimation in comparison with an alternative. The alternative method used here is that proposed by Jiang *et al.* [15], which assumes known material reflectance for every pixel and a global CIE standard daylight illuminant. This method also constrains spectral sensitivity functions to a two-dimensional subspace spanned by the principal components of a library of camera sensitivity functions. Later on in the section, we demonstrate the application of our method to camera simulation, and colour transfer across camera spectral sensitivity functions.

To generate synthetic input for validation purposes, we have simulated colour images from a spectral reflectance image of the semi-gloss Xrite ColorChecker, which comprises 140 colour patches, and a Macbeth ColorChecker with 24 colour tiles. This imagery was captured using a hyperspectral camera equipped with an Liquid Crystal Tunable filter resolving wavelengths in the visible range, i.e. between 400 nm and 720 nm, at 10 nm steps. The chart reflectance is computed as the ratio of the measured irradiance to that falling on a white patch on the chart.

Subsequently, we render the images of the colour charts using two datasets of spectral sensitivity functions acquired by Jiang *et al.* [15] and Zhao *et al.* [19] from over 40 commercial digital camera models. To generate the colour images, we employ two representative illuminants that cover the full extent of the visible spectrum, including an incandescent light and the natural sunlight. Throughout our experiments, we have set the above algorithm parameters as follows,  $\alpha_L = 50, \alpha_Q = 0.5, \beta_Q = 1, \gamma_Q = 1$  and  $\epsilon = 0.05$ .

In Tables I and II, we show the mean root-mean-square (RMS) errors for the spectral sensitivity functions in the

Camera model	Our method			Jiang et al. [15]		
	Red	Green	Blue	Red	Green	Blue
NikonD40	<u>0.15</u>	<u>0.1</u>	<u>0.11</u>	0.082	0.03	0.095
NikonD700	0.063	0.074	0.056	<b>0.072</b>	<b>0.029</b>	<b>0.04</b>
NokiaN900	0.11	0.1	0.075	<u>0.12</u>	<u>0.1</u>	<u>0.18</u>
PentaxK5	<b>0.053</b>	<b>0.085</b>	<b>0.037</b>	0.056	0.047	0.05
Average	0.085 ± 0.0309	0.081 ± 0.0217	0.071 ± 0.027	0.088 ± 0.0255	0.049 ± 0.0257	0.079 ± 0.0497

TABLE I. RMS ERRORS FOR THE SPECTRAL SENSITIVITY FUNCTIONS IN THE CAMERA DATASET COLLECTED BY JIANG *et al.* [15] AVERAGED OVER ALL THE ILLUMINATION CONDITIONS.

Camera model	Our method			Jiang et al. [15]		
	Red	Green	Blue	Red	Green	Blue
Kodak DCS 460	<u>0.18</u>	<u>0.065</u>	<u>0.13</u>	<u>0.19</u>	<u>0.082</u>	<u>0.2</u>
Canon 400D	<b>0.058</b>	<b>0.043</b>	<b>0.047</b>	<b>0.066</b>	<b>0.042</b>	<b>0.067</b>
Average	0.11 ± 0.0641	0.066 ± 0.0272	0.086 ± 0.0394	0.12 ± 0.0645	0.073 ± 0.0249	0.1 ± 0.0509

TABLE II. RMS ERRORS FOR THE SPECTRAL SENSITIVITY FUNCTIONS FOR CAMERA DATASET COLLECTED BY ZHAO *et al.* [19] AVERAGED OVER ALL THE ILLUMINATION CONDITIONS.

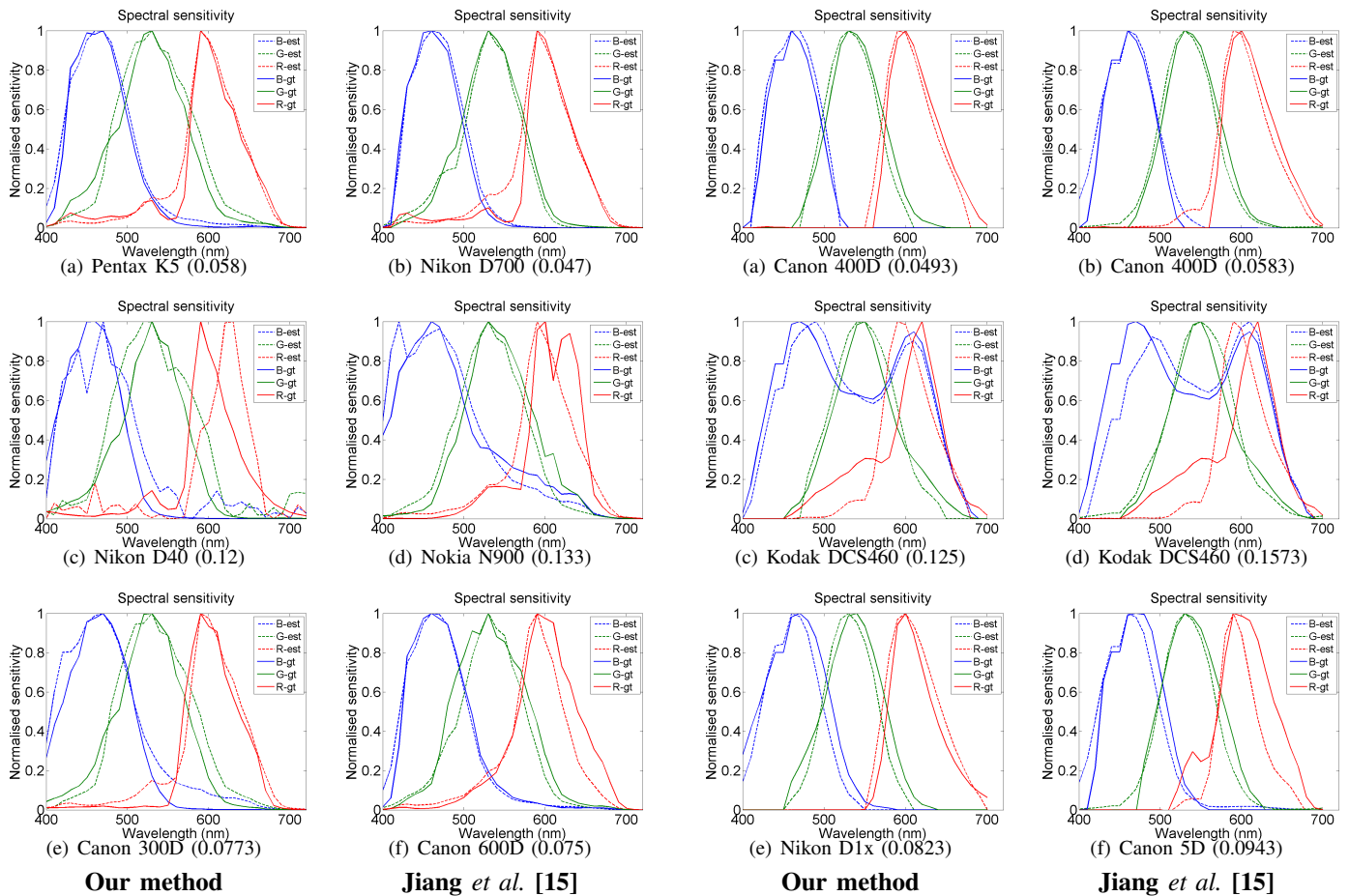


Fig. 1. The spectral sensitivity functions in the dataset collected by Jiang *et al.* [15], with the corresponding average RMS errors across the colour channels in parentheses.

datasets in [15] and [19], respectively. The errors resulting from our method and the alternative are presented per camera and colour channel, averaged over all the illumination conditions. Here, for the sake of brevity, we only show the error measure for the camera models that yield the most (in bold) and the least accurate (underlined) estimates for each method. From the tables, we can observe that the performance of our method on Jiang *et al.*'s dataset is largely comparable to the alternatives. Meanwhile, our method consistently outperforms

Fig. 2. The spectral sensitivity functions in the dataset collected by Zhao *et al.* [19], with the corresponding average RMS errors across the colour channels in parentheses.

the alternative when applied to Zhao *et al.*'s dataset, with the mean RMS errors approximately 10% lower than those produced by the alternative. Interestingly, both our method and the alternative yield the highest and lowest performance on the same cameras, i.e. the Canon 400D and Kodak DCS460 camera. These results suggest that although our algorithm makes weaker assumptions on the illuminant than the alternative, its performance is at least comparable or better than the alternative. Note that our optimisation framework can be

treated as generalisation of the alternative, where the additional constraints on the colour matching functions (including the smoothness constraint and the weighting of bands) help guide the estimates closer to the ground truth.

In Figures 1 and 2, we plot the ground truth spectral sensitivity functions (in solid traces) and the estimates (in dashed lines) produced by the two methods under study for the two camera datasets. In the plots, the estimates for our method and the alternative are shown in the left-hand and right-hand column, respectively. From top-to-bottom, we show the best, worst and average estimates for each method, respectively. We note that the RMS differences between the estimates and the ground truth (in the parentheses under the plots) reflect the numerical results in Tables I and II.

Next, we employ the image formation model in Equation 2 to render spectral images in the colour depicted by the camera sensitivity functions resulting from the two methods above. This simulation takes input from the dataset of spectral reflectance images acquired by Foster *et al.* [21]. In Figure 3, we show the simulated colour for a sample scene using the most and least accurate estimate for the spectral sensitivity function produced by our method over the two camera datasets above. These renderings correspond to the Pentax K5 and the Kodak DCS460 cameras. In the figure, the first, second and fourth columns show the simulated colours using the ground truth spectral sensitivity functions, and those estimated by our method and Jiang *et al.*'s method, respectively. In the third and last columns, we visualise the rendering error for our estimate and the alternative. The error maps are scaled up by a factor of 5 for the sake of clarity of presentation.

Note that, our error for the Pentax K5 camera (in the first row) is almost negligible while that for the alternative is visible in the well-lit areas. On the other hand, both error maps for the Kodak DCS460 camera in the second row exhibit noticeable errors in various parts. This is consistent with the results above, where the sensitivity function estimation for the Pentax K5 is much more accurate than that for the Kodak DCS460.

Lastly, we utilise the estimated spectral sensitivity functions for the task of colour transfer between camera models. In particular, given a real-world image captured by a known camera model, we transfer the input colour to that perceived by a target spectral sensitivity function or the human standard observer. This is, in effect, a linear transformation to map the input colour to that corresponding to a target spectral sensitivity function. Here, suppose that the colour matching functions corresponding to the CIE 1931 2° Standard Observer [22] is  $\hat{\mathbf{Q}}$ . We denote the camera colour matching functions across the three colour channels as  $\mathbf{Q}$  and the image colour as an  $m \times 3$  matrix  $\mathbf{I}$ . After normalising  $\mathbf{Q}$  and  $\hat{\mathbf{Q}}$ , we obtain the colour vector observed by the target colour matching function as  $\mathbf{I}\mathbf{Q}^\dagger\hat{\mathbf{Q}}\text{diag}([\sigma_R, \sigma_G, \sigma_B])$ , where  $\sigma_c$  is a normalising constant for the channel  $c$ .

In Figure 4, we show input images captured by a Nikon D80 and a Nikon D5100 in the first and third columns. The second and fourth columns depict the colour images resulting from the transfer matrix between the colour matching functions of the above cameras and the CIE standard observer's functions [22]. We note the similarity between the hues transferred from images captured by the two camera

models under the same illumination. Furthermore, the transfer operation only modifies the chrominance of the image while preserving the luminance. This is expected since the spectral sensitivity functions are independent from the image intensity. We also notice that both the Nikon D80 and Nikon D5100 sensors are more sensitive to the long wavelengths and less sensitive to the short wavelengths than the eye. Thus, the images they capture exhibit a stronger red tone and a milder blue tone than perceived by the human eye.

## V. CONCLUSION

We have presented a method for estimating the spectral sensitivity function of a digital camera from a single image of a colour chart captured under an unknown illuminant with a smooth spectrum. We have turned this ill-posed problem into a well-formed one by introducing constraints on the spectral sensitivity function and the illuminant power spectrum. These constraints aim to model the characteristic variation of both the illuminant and the spectral sensitivity functions over the spectral domain. Our experiments show favourable results over an alternative [15] when applied to 40 commercially available digital cameras. We have also illustrated the utility of our method for the purposes of colour simulation and colour transfer.

## ACKNOWLEDGMENT

NICTA is funded by the Australian Government as represented by the Department of Broadband, Communications and the Digital Economy and the Australian Research Council through the ICT Centre of Excellence program.

## REFERENCES

- [1] D. H. Brainard and A. Stockman, *Colorimetry*. McGraw-Hill, 1995.
- [2] G. D. Finlayson and M. S. Drew, "The maximum ignorance assumption with positivity," in *Proceedings of the IS&T/SID 4th Color Imaging Conference*, 1996, pp. 202–204.
- [3] P. Longere and D. H. Brainard, "Simulation of digital camera images from hyperspectral input," in *Vision Models and Applications to Image and Video Processing*, C. van den Branden Lambrecht, Ed. Kluwer, 2001, pp. 123–150.
- [4] T. Ejaz, T. Horiuchi, G. Ohashi, and Y. Shimodaira, "Development of a camera system for the acquisition of high-fidelity colors," *IEICE Transactions on Electronics*, vol. E89–C, no. 10, pp. 1441–1447, 2006.
- [5] W. S. Stiles and J. M. Burch, "Interim report to the Commission Internationale de l'Éclairage Zurich, 1955, on the National Physical Laboratory's investigation of colour-matching," *Optica Acta*, vol. 2, pp. 168–181, 1955.
- [6] H. T. Lin, S. J. Kim, S. Süsstrunk, and M. S. Brown, "Revisiting radiometric calibration for color computer vision," in *ICCV*, 2011, pp. 129–136.
- [7] G. Wyszecki and W. Stiles, *Color Science: Concepts and Methods, Quantitative Data and Formulae*. Wiley, 2000.
- [8] P. L. Vora, J. E. Farrell, J. D. Tietz, and D. H. Brainard, "Linear models for digital cameras," in *Proceedings of the IS&T's 50th Annual Conference*, 1997, pp. 377–382.
- [9] G. Finlayson, S. Hordley, and P. Hubel, "Recovering device sensitivities with quadratic programming," in *Proceedings of the IS&T/SID Color Imaging Conference*, 1998, pp. 90–95.
- [10] P. Urban, M. Desch, K. Happel, and D. Spiehl, "Recovering camera sensitivities using target-based reflectances captured under multiple led-illuminations," 2010, pp. 9–16.
- [11] M. Rump, A. Zinke, and R. Klein, "Practical spectral characterization of trichromatic cameras," in *Proceedings of the 2011 SIGGRAPH Asia Conference*, 2011, pp. 170:1–170:10.

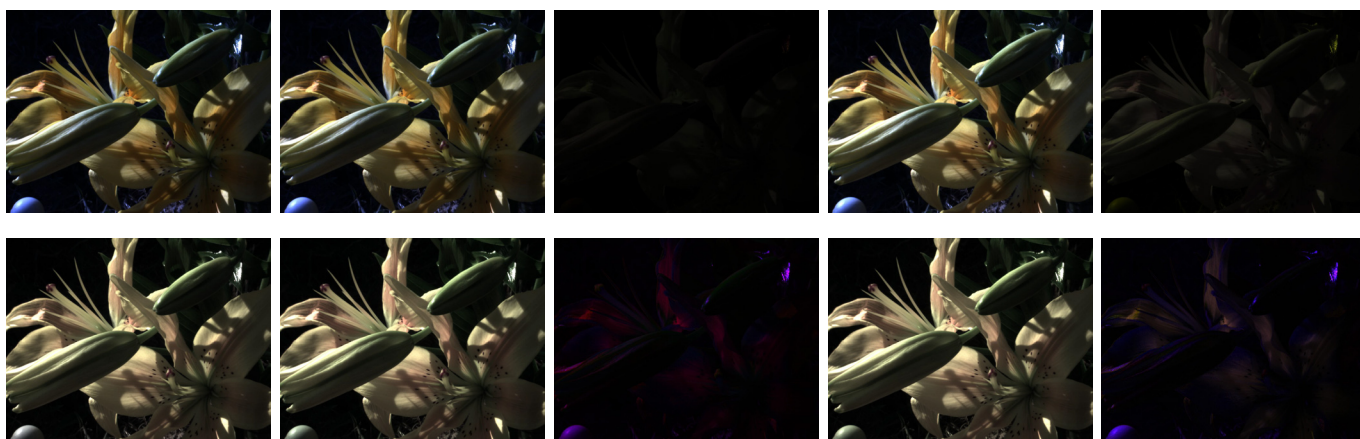


Fig. 3. Colour simulation results for a Pentax K5 (top row) and a Kodak DCS460 (bottom row) camera. First, second and fourth columns: Simulated colours using the ground truth spectral sensitivity functions, those estimated by our method and Jiang *et al.*'s [15], respectively. The rendering error with respect to the ground-truth for our approach is shown in the third column and for Jiang *et al.*'s method is shown in the fifth column.



Fig. 4. The transfer of colours from the spectral sensitivity functions of a camera to the CIE 1931 colour matching function for the 2° Standard Observer. First and third columns: Input images captured by a Nikon D80 and a Nikon D5100. Second and fourth columns: the images with their colour transferred to the standard colour matching function.

- [12] S. Han, Y. Matsushita, I. Sato, T. Okabe, and Y. Sato, "Camera spectral sensitivity estimation from a single image under unknown illumination by using fluorescence," in *Computer Vision and Pattern Recognition*, 2012.
- [13] K. Barnard and B. Funt, "Camera characterization for color research," *Color Research & Application*, vol. 27, no. 3, pp. 152–163, 2002.
- [14] R. Kawakami, H. Zhao, R. T. Tan, and K. Ikeuchi, "Camera spectral sensitivity and white balance estimation from sky images," *International Journal of Computer Vision*, vol. 105, no. 3, pp. 187–204, 2013.
- [15] J. Jiang, D. Liu, J. Gu, and S. Susstrunk, "What is the space of spectral sensitivity functions for digital color cameras?" in *Proceedings of the 2013 IEEE Workshop on Applications of Computer Vision (WACV)*, ser. WACV '13, 2013, pp. 168–179.
- [16] J. Nakamura, *Image Sensors and Signal Processing for Digital Still Cameras*, ser. Optical Science and Engineering. Taylor & Francis/CRC Press, 2006.
- [17] C. L. Lawson and R. J. Hanson, *Solving Least Squares Problems*. Prentice-Hall, 1974.
- [18] J. Zhang, B. Rivard, and A. Sanchez-Azofeifa, "Derivative spectral unmixing of hyperspectral data applied to mixtures of lichen and rock," *IEEE Transactions on Geoscience and Remote Sensing*, vol. 42, no. 9, pp. 1934 – 1940, 2004.
- [19] R. T. T. Hongxun Zhao, Rei Kawakami and K. Ikeuchi, "Estimating basis functions for spectral sensitivity of digital cameras," in *Meeting on Image Recognition and Understanding*, 2009.
- [20] R. H. Byrd, M. E. Hribar, and J. Nocedal, "An interior point algorithm for large-scale nonlinear programming," *SIAM Journal on Optimization*, vol. 9, no. 4, pp. 877–900, 1999.
- [21] D. H. Foster, S. M. Nascimento, and K. Amano, "Information limits on neural identification of colored surfaces in natural scenes," *Visual Neuroscience*, vol. 21, pp. 331–336, 2004.
- [22] CIE, *Commission Internationale de l'Éclairage Proceedings, 1931*. Cambridge University Press, Cambridge, 1932.